Supplementary Material

Evolution of the SARS-CoV-2 main protease under fitness constraints imposed by folding stability and activity

The supplementary material includes Figures S1-S3.

Supplementary Figures

Figure S1. Backbone RMSD time series for wild-type and mutant variants of the SARS-CoV-2 Mpro bound to the natural substrates during 10-ns molecular dynamics simulations. RMSD shown for the substrates nsp4–5 (A), nsp5–6 (B) and nsp10–11 (C). Each variant-substrate complex was simulated in three independent replicates and each presents an individual molecular dynamics trajectory.

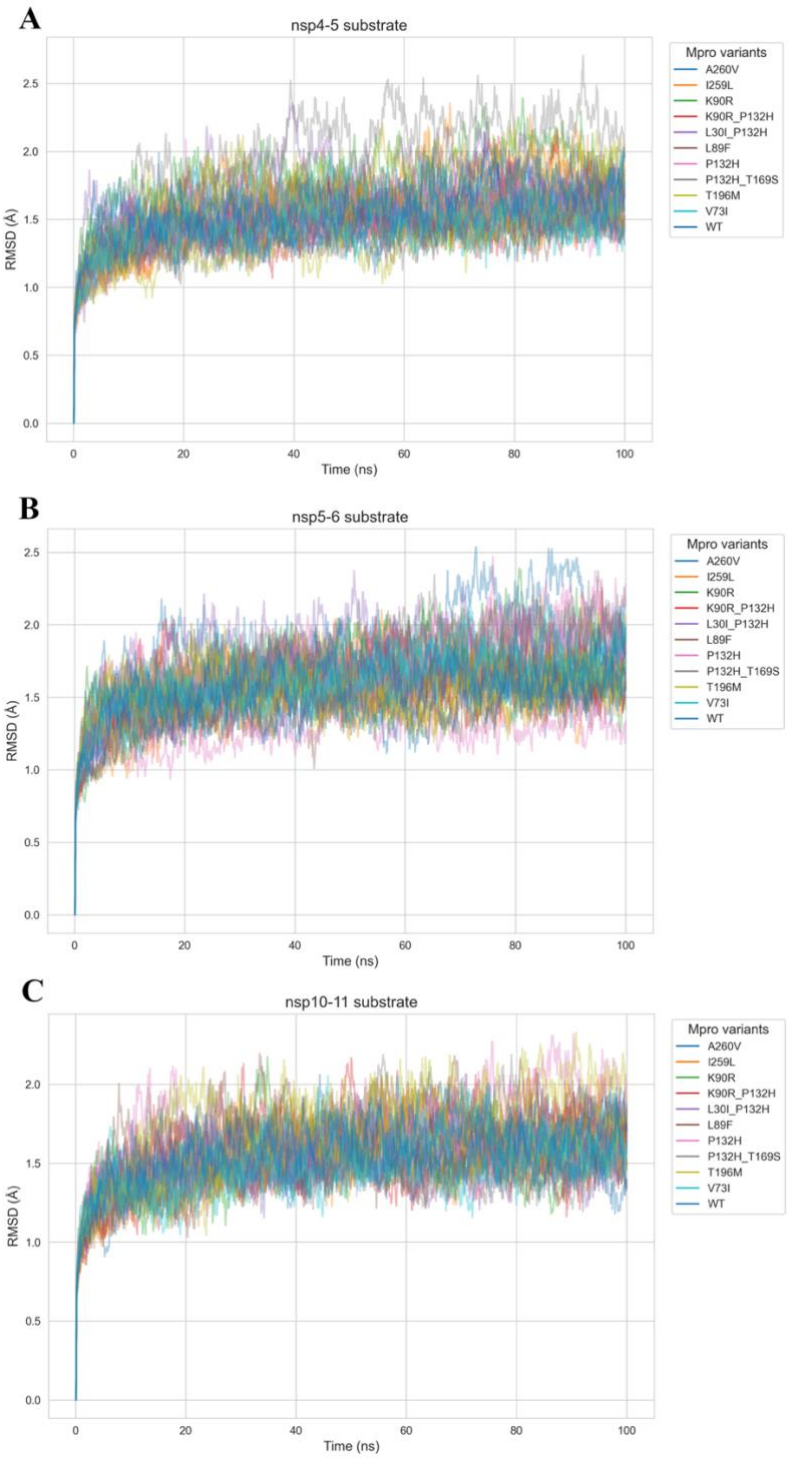

Figure S2. Binding energies of individual substrate residues with SARS-CoV-2 Mpro mutant variants relative to the WT variant. Differences in terms of binding energy (ΔΔG, shown in the legend) for each residue of the natural substrates [nsp4-5 (A), nsp5-6 (B) and nsp10-11 (C)] in complexes with the Mpro mutant variants relative to the WT variant. The color scale indicates lower (red) or higher (blue) binding energy relative to the WT variant.

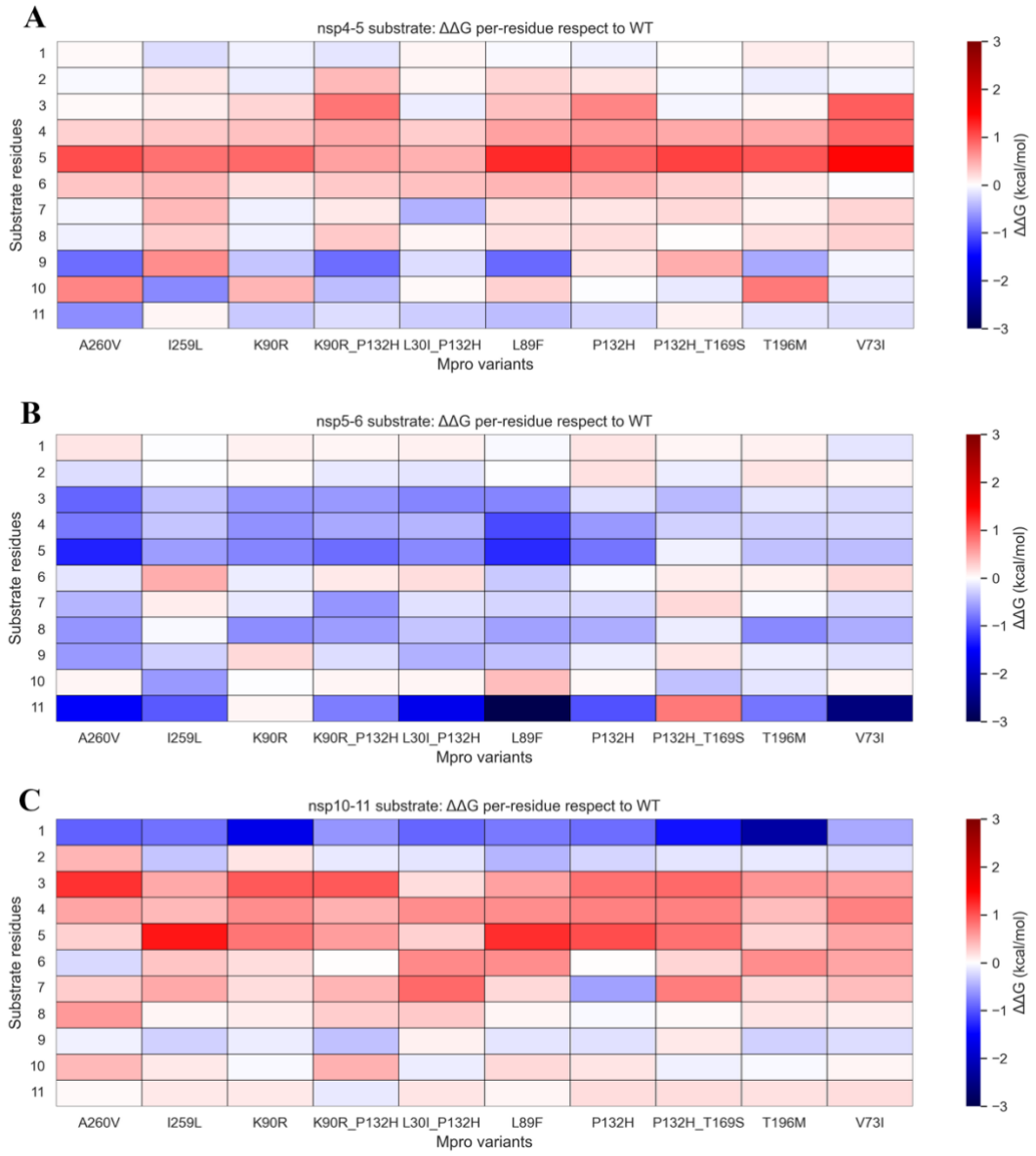

Figure S3. Hydrogen-bond occupancy of individual substrate residues in complexes with SARS-CoV-2 Mpro mutant variants relative to the WT variant. Differences in terms of hydrogen-bond prevalence (ΔHB) for each residue of the natural substrates [nsp4-5 (A), nsp5-6 (B) and nsp10-11 (C)] in complexes with the Mpro mutant variants relative to the WT variant. The color scale indicates lower (red) or higher (blue) hydrogen-bond occupancy relative to the WT variant.